Accepted Manuscript

Nanoscale frictional properties of ordered and disordered MoS_2

Elisabetta Serpini, Alberto Rota, Sergio Valeri, Egor Ukraintsev, Bohuslav Rezek, Tomas Polcar, Paolo Nicolini

PII: S0301-679X(19)30118-5

DOI: https://doi.org/10.1016/j.triboint.2019.03.004

Reference: JTRI 5646

To appear in: *Tribology International*

Received Date: 19 December 2018

Revised Date: 22 February 2019

Accepted Date: 2 March 2019

Please cite this article as: Serpini E, Rota A, Valeri S, Ukraintsev E, Rezek B, Polcar T, Nicolini P, Nanoscale frictional properties of ordered and disordered MoS_2, *Tribology International* (2019), doi: https://doi.org/10.1016/j.triboint.2019.03.004.

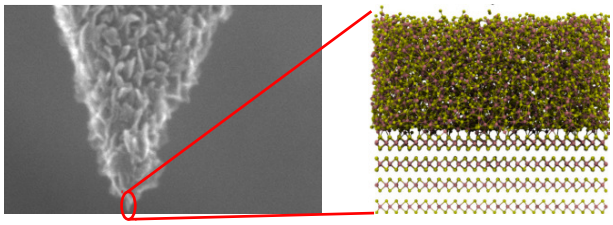

The tribological properties of MoS_2 at nanoscale are studied by means of AFM/LFM experiements and MD simulations.

Nanoscale frictional properties of ordered and disordered MoS_2

Elisabetta Serpini[a,*], Alberto Rota[b], Sergio Valeri[a,b,c], Egor Ukraintsev[d,e], Bohuslav Rezek[d,e], Tomas Polcar[e], Paolo Nicolini[e,*]

[a] *Dipartimento di Scienze Fisiche, Informatiche e Matematiche, Università di Modena e Reggio Emilia, Via Campi 213/A, 41125 Modena, Italy*
[b] *Centro Interdipartimentale per la Ricerca Applicata e i Servizi nella Meccanica Avanzata e nella Motoristica Intermech-Mo.Re., Università di Modena e Reggio Emilia, Via Vignolese 905/b, 41125 Modena, Italy*
[c] *Istituto CNR-NANO S3, Via Campi 213/A, 41125 Modena, Italy*
[d] *Institute of Physics, ASCR, Cukrovarnická 10, 162 00 Prague 6, Czech Republic*
[e] *Faculty of Electrical Engineering, Czech Technical University, Technická 2, 166 27 Prague 6, Czech Republic*

Abstract

The present work aims to understand the sliding of ordered/disordered molybdenum disulfide against itself by combination of nanoscale sliding experiments and atomistic simulations. Tribological experiments were performed using lateral force microscopy with tips covered by a thin sputtered MoS_2 film. Nanoscale contact area between the MoS_2-coated tips and MoS_2 samples opened up the possibility for close comparison with classical molecular dynamics simulations. Our simulations replicated well the coefficient of friction obtained by experiments for various contact conditions and shed light on nanoscale sliding of both crystalline and amorphous MoS_2. Experimental sliding at humid environment demonstrated detrimental effect of water molecules on friction. However, such effect was much less pronounced when compared to that observed in macroscopic sliding experiments.

Keywords: molybdenum disulfide, atomic force microscopy, friction, molecular dynamics simulations

1. Introduction

Molybdenum disulfide (MoS_2) is a well-known lamellar solid lubricant first employed in the aerospace industry in the 1960s in the form of films applied to sliding counterparts[1–5]. MoS_2 provides the best lubricating capability in vacuum or inert atmospheres, whereas humidity proved to be detrimental for both low friction and wear rates[1, 3, 5–8]. The interest was mainly focused on thick films (1 μm and above), at first produced by powder burnishing and then by physical vapor deposition (PVD) methods, which are still under

*Corresponding authors
Email addresses: elisabetta.serpini@unimore.it (Elisabetta Serpini), nicolpao@fel.cvut.cz (Paolo Nicolini)

development nowadays. PVD coatings proved to be the best solution for solid lubrication in vacuum for many years. Thickness, together with chemical, morphological and ultimately frictional properties can be tailored by simply modifying the deposition parameters and coefficients of friction (COFs) as low as 0.01 have been measured[3–12].

More recently, MoS_2 in various shapes (platelets, nanotubes, nano-onions) started to be utilized as additives in lubricant oils as well[13]. About ten years ago, an interest in thin films was revived due to possible applications in micro or nano electro-mechanical (MEMS/NEMS) devices[14, 15]. Along with the progressive miniaturization of the lubricating elements, researchers started to investigate the micro and nanostructure of these lubricating elements[16]. MoS_2 nanostructured materials are widely used in energy and environmental applications[17]. MoS_2 containing self-lubricating composites were reviewed in Ref. [18].

Even though the macroscopic properties of thick films are well known, the intrinsic friction mechanisms are still to be unraveled. For thick films, three main conditions need to be satisfied in order to reach ultra-low friction: a transfer film must build up on the counterpart in order to have sliding of MoS_2 against itself; MoS_2 grains at the interface must be either re-oriented or newly formed with the (0001) basal planes parallel to the sliding direction; and, most importantly, the presence of contaminants must be minimized. This last condition relates both to contaminants contained in the coating itself (for example, oxygen is often present either as molybdenum oxide and/or as an interstitial or substitutional species), and to atmospheric contaminants[7, 19, 20]. The debate whether the degradation of MoS_2 lubricating properties is due either to oxidation or water molecules physisorption started along with the systematic study of the material itself[1, 21–25] and only recently reached a conclusion[26–29]. Khare *et al.*[26, 27] and Serpini *et al.*[28] demonstrated that the most detrimental effect at temperatures below 100 °C to MoS_2 lubricity was due to the physisorption of water molecules. The former team examined the case of thin films, the latter thick ones. In fact, adsorption of water molecules was identified as the main contributor to friction increase in the case of $MoSe_2$ tribolayer formed at sliding interface of Mo-Se-C sputtered coating, so it is a general feature of transition metal dichalcogenides from Mo/W S/Se family[30].

The ability to prepare 2D materials based on transitional metal dichalcogenides opened new possibilities for nanoscale tribological research of MoS_2. We can now measure directly friction between two MoS_2 2D flakes[31]. Unfortunately, theoretical tools to predict friction behavior are still under development. *Ab initio* simulations have been employed in recent years to investigate friction of single crystal MoS_2[32–35], but they fail to represent realistic sliding scenarios (*e.g.* they do not include defects/contaminations, thermal noise, native roughness of 2D MoS_2 flakes placed on a substrate, etc.). Moreover, the main limitation of *ab initio* approaches is the absence of dynamics, *e.g.* the shear strength which can be obtained is related to static friction only. Molecular dynamics (MD) simulations have greatly contributed to the understanding of the phenomena that take place at nanoscale in tribological conditions[36]. For example, focusing on molybdenum disulfide, the sliding dynamics of a small flake on top of a large substrate has been studied computationally with particular regard to the commensuration of the two objects[37]. In the paper, a force field

for MoS_2 composed of Buckingham-like terms, Morse pair potential, harmonic angle bending contributions and fixed-charges electrostatics has been employed. The incommensurate structures showed superlubrication due to cancellation of the atomic forces in the sliding direction, whilst, in commensurate situations, friction turned out to be 100 times larger than in the former case. Dallavalle *et al.* studied the tribological behavior of MoS_2 platelets and nanotubes[38]. They developed and used a simple force field made of Lennard-Jones interactions augmented with variable atomic charges. The authors studied the lubrication mechanism of nanotubes, also calculating the friction coefficient values by using Amontons' law and Green-Kubo relations. For nanotubes, friction was one order of magnitude lower than in the layered systems. More recently, a ReaxFF model has been proposed[39] and used to study oxidation and oxygen diffusion of MoS_2 surfaces for highly ordered crystalline film and a partially amorphous/nanocrystalline coating[40]. MD results confirmed that atomic oxygen readily reacts at room temperature with MoS_2 surfaces and that the diffusion of oxygen within the film decreases with the number of potentially active edge sites. Among classical interaction potentials, the ReaxFF description is probably the more complete, taking into account, among the many *ad hoc* contributions, bond-order-based terms and electrostatics with variable charges[41].

The aim of the present work is to remedy, at least partially, the lack of systematic study of the tribological properties of MoS_2 at the nanoscale, both from the experimental and the computational point of view. To represent various sliding scenarios, two MoS_2 materials have been tested – disordered sputtered MoS_2 and molybdenite single crystal. Atomic force microscopy (AFM) in the lateral force mode (LFM) was used as the experimental sliding device. Traditional use of Si tips is of very limited value despite the expected material transfer from the substrate to the tip; in particular, the transfer film on the AFM tip during single crystal siding is not guaranteed. Therefore, we covered the tips by a thin sputtered MoS_2 film, which eliminates long running-in phases and assure self-mating contact of MoS_2. In this paper, together with AFM sliding experiments, we exploit the ReaxFF parameterization in order to study the frictional properties at nanoscale of crystalline and highly disordered MoS_2 samples.

2. Experimental details

2.1. MoS_2 coatings preparation

The substrate consists of 1x1 cm^2 Si(111) single crystal covered by native oxide. After cleaning in acetone + isopropanol, the substrate was coated by 200 nm MoS_2 film by means of radio frequency (RF) magnetron sputtering technique from a 99.99 % purity MoS_2 target. The base pressure in the deposition chamber was 10^{-6} mbar and 10^{-3} mbar Ar^+ partial pressure. During deposition a 150 W RF power were applied to the target, both for conditioning (15') and for deposition; neither heating nor bias voltage were applied to the substrate. These systems served as samples for AFM investigation. New and unused AFM tips (Veeco, 70 kHz resonance frequency, 3 N m^{-1} force constant) where covered by sputtered MoS_2 with different thicknesses, following the same recipe (only the duration of the deposition process was varied).

2.2. Friction measurements

AFM measurements were performed on a NT-MDT NTEGRA AFM using silicon cantilevers (force constant 3 N m^{-1}) with deposited MoS_2 disordered coatings as described above. Samples were the previously described coatings and MoS_2 single crystals (molybdenite, SPI Supplies). Friction measurements were performed in humid and dry nitrogen atmospheres. In particular, dry nitrogen represents an inert atmosphere better suited for studying intrinsic MoS_2 friction mechanism; moreover, it allows direct comparison with our MD simulations. For measurements in dry conditions, N_2 was fluxed in the chamber down to 10 % relative humidity (RH), checking RH level through a dedicated sensor. In the case of humid nitrogen, the gas was first fluxed inside a bottle containing de-ionized water and then the mixture was fluxed inside the lid covering the AFM. The measurements were performed once the RH level had stabilized above a 90 % RH value.

The morphological characteristics of the surface were first checked by AFM working in intermitting contact mode on a flat area of 5x5 μm^2. All presented friction curves and analyzed data were obtained on horizontal areas (slope < 1 %). Measurements on nonhorizontal areas gives non-linear dependencies, probably due to non-ideal cancelation of topography features. The friction characterization were performed working in contact mode forcing the tip to slide on a single 5 μm line, with 1 $\mu m\ s^{-1}$ scanning speed and with a resolution of 512 px/line. The spring normal and lateral constants of the cantilever were determined using the Sader method[42, 43]. The geometrical characteristics of the cantilever and of the tip were measured by means of SEM, while the proper vibration frequencies were detected in air by means of AFM.

The friction force was measured measuring the torsional deflection during trace and retrace scans, representing the trace-minus-retrace signal expressed in Newton[44, 45]. The tribological characterization consists in the detection of the friction force during a load-decreasing ramp, starting at approximately 1.5 μN load down to the pull-of-force; the applied load was changed every 20 lines. The coefficient of friction was calculated as the slope of the friction force vs load curve. This method was repeated several times in different parts of the sample using the same tip, in order to increase the statistics.

3. Computational details

In order to understand the processes that take place at the atomic level, a set of MD simulations were performed by means of the LAMMPS package[46]. A time step of 0.1 fs was employed in all simulations. Atomic interactions were calculated exploiting the recently published ReaxFF potential for MoS_2[39]. This force field is reactive (*i.e.*, it can properly model the formation and breaking of chemical bonds) and its performance was tested in order to assess the accuracy in predicting structural and energetic properties relevant to this study (see Section S4 of the Supporting Information for more details). The 2H crystal phase was selected as starting configuration (atomic positions in the unit cell were obtained from X-ray diffraction experiments[47]). The hexagonal cell was then transformed into an orthogonal one by using the scheme described elsewhere[48] and replicated 12, 24 and 2 times in the x, y and z directions respectively. The structure was then optimized through an

energy minimization by means of the conjugate gradient method. The atomic positions and the box size and shape were allowed to vary during this step. The amorphous configurations were produced as follows. The box sizes were kept the same as in the optimized cell in the x and y directions. The value of the box size in the z direction was instead set in order to match the experimental value of the coating density (*i.e.*, 3.10 g cm^{-3}, see below). The system was then heated at 5000 K and at constant volume for 20 ps, controlling the temperature via a Nosé-Hoover[49, 50] chain of thermostats leading to the complete melting of the sample. The system was then further equilibrated at 5000 K for 100 ps, and, after that, the temperature was decreased to 300 K with a cooling rate of 2.35 K fs^{-1} and at constant volume[51]. The latter two steps were repeated five times in order to sample five independent configurations relevant to represent the amorphous phase. These configurations were then processed in order to create a slab geometry, namely we inserted 20 Å of vacuum in the z-direction thus preventing interactions between replicas due to periodic boundary conditions. The samples were further equilibrated at 300 K controlling the temperature as done before for 6.5 ns. Total energy of the systems was monitored at this stage and simulations continued until a stable value was reached.

Two kinds of computational setup were then prepared: the first one is obtained by putting into contact two amorphous slabs (below denoted as "A-A") and the second one by assembling an amorphous slab with a crystalline sample ("A-C")[1]. 20 Å of vacuum in the z-direction were inserted in order to prevent interactions between replicas and an energy minimization using the conjugate gradient method was then performed. Within these configurations two regions of thickness 7 Å were defined (one at the top and one at the bottom of the system) and they were treated as rigid bodies for the subsequent simulations. The assembled systems were finally equilibrated for 1 ns at room temperature by imposing different normal loads (*i.e.*, 3, 4, 5, 6, 7 and 8 GPa) to the top region until a stable value of the system's total energy was reached. During this stage, the position of the atoms belonging to the top group were kept fixed in the x and y directions, whilst atomic positions of the bottom group were kept totally frozen. The imposed normal loads were chosen in order to match as closely as possible the regime of contact pressures studied by LFM experiments[2]. The final configurations contain 13824 atoms and the simulation boxes had sizes of 66.2 and 76.4 Å in the x and y directions respectively (box size in the z direction varies from sample to sample and it was about 105 and 85 Å for the A-A and A-C setups respectively).

These equilibrated configurations were the starting points of the subsequent non-equilibrium simulations. To mimick tribological conditions, a normal load and a constant speed of 5 m s^{-1} along the x direction were enforced within the top group, while the atoms belonging to the bottom group were kept frozen. The temperature was kept constant at 300 K for 1 ns. Atomic positions, velocities and forces were stored every 50 fs for the subsequent data analysis. Lateral forces along the sliding direction were then calculated by summing the

[1]The same labels are used in the next sections to denote respectively sliding of MoS_2-covered tips against a MoS_2-coated substrate and against a MoS_2 single crystal.

[2]The conversion between normal load and maximum contact pressure was done by using the Hertz model[52] for a sphere of radius 80 nm and a half-space and by employing the values of the elastic modulus and Poisson ratio for crystalline MoS_2 taken from literature[53].

atomic contributions over all atoms belonging to the top group and then averaged over part of the MD trajectory.

4. Results

4.1. MoS_2 coatings characterization

4.1.1. Films

The surface morphology, studied with scanning electron microscopy with field emission guns (SEM-FEG), revealed the presence of needle-like structures several tens of nm long and less than 10 nm thick (see Fig. S1 in the Supporting Information), similar to structures previously seen in the literature[6]. However, although the needles were traditionally considered as the top of the columnar structure, in this case focused ion beam cross-section did not evidenced the presence of columns in the film. In fact, the film appears homogeneous and dense, similar to that described by Spalvins[3, 4].

Density of the coating was estimated to be $3.5 \cdot 10^{22}$ at. cm^{-3} (corresponding to 3.10 g cm^{-3}) with the Rutherford backscattering technique. The value is in the range of densities observed experimentally in sputtered coatings (0.77 - 4.07 g cm^{-3})[6]. The X-ray diffraction characterization showed the presence of broad peaks related to (100) crystalline orientation (see Fig. S2 in the Supporting Information). This confirm the polycrystalline nature of the film, with nanometric crystallites randomly oriented. Finally, the chemical composition of the films was measured by Auger electron spectroscopy. The films were found to be close to stoichiometry (see Tab. S1 in the Supporting Information).

4.1.2. AFM tips

AFM silicon tips were imaged with SEM-FEG prior to and post MoS_2 deposition. Several tips were coated with the same film thickness. Fig. 1 shows SEM-FEG images of the tip effectively used in AFM measurements prior to (Fig. 1a) and after the deposition (Fig. 1b) of a 100 nm-thick MoS_2 film.

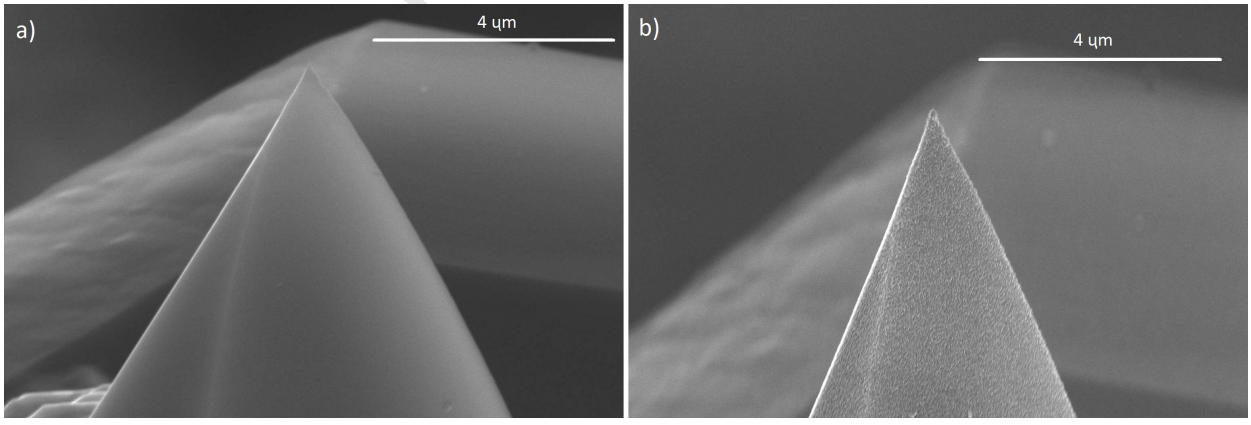

Figure 1: SEM-FEG images (40 kX magnification) of the tip utilized in this work, prior to (a) and post (b) 100 nm-thick MoS_2 film deposition.

Upon closer inspection of the tip apex (see Fig. 2a), it is possible to observe the needle-like structures previously mentioned, with needles protruding outside the coating. After the AFM measurements, the tip was imaged again to check the continuity of the residual film (Fig. 2b).

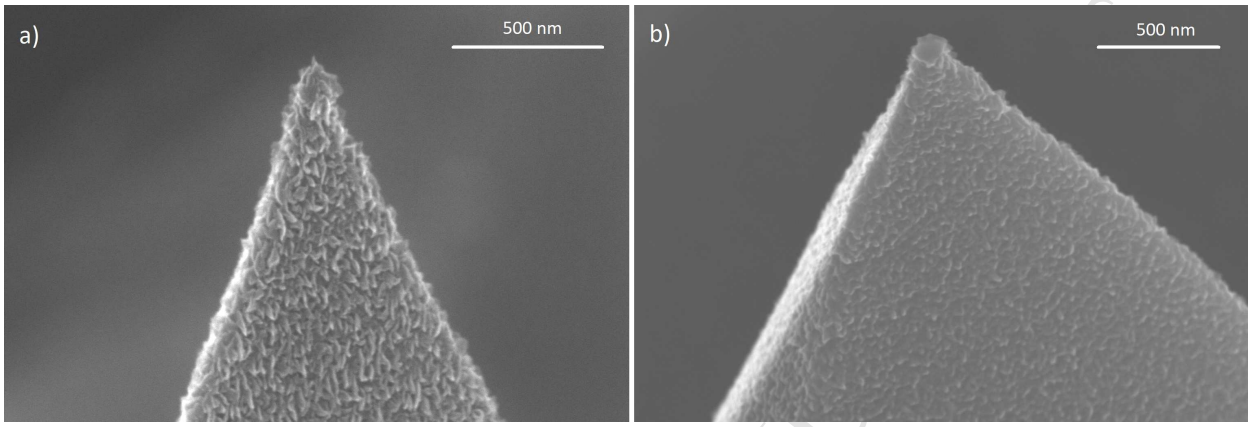

Figure 2: SEM-FEG images of the AFM tip utilized in this work, sputter-deposited with 100 nm MoS_2 film, prior to the measurements (a – 200 kX magnification) and after (b – 160 kX magnification). Needle-like structures are visible on the tip apex and get flattened after the friction tests, however the Si underneath is not uncovered.

The surface of MoS_2-coated tips were morphologically very similar to that of the films deposited on Si single crystal, indicating that the MoS_2 tip deposition was successfully. The coated tips were chemically characterized by Energy-dispersive X-ray (EDX) spectroscopy, evidencing the presence of the Mo/S typical peaks. In the case of EDX, the Mo and peaks are very close to each other and it is not possible to obtain a precise chemical analysis, but anyway they are the proof of the presence of the coating (see Fig. S5 in the Supporting Information).

4.2. LFM measurements

The present work always refers to tip covered by 100 nm MoS_2, being the most reliable results (see Fig. 1). Different coating thickness were deposited as well, but they led to unstable behaviour (see Section S2 in the Supporting Information). Further, the same tip was used in all the tests presented, in order to minimize the effect of the tip shape. In fact, we observed that the tip shape, after an initial flattening due to wear, changed very slowly during the sliding.

The friction curves from identical tests are shown in the Supporting Information (Fig. S8-S11) to show the related data dispersion. In all tests it is evident the linear relationship between the lateral force and the load, indicating that this tribological system can be described by the Amontons' law:

$$F_f = \mathrm{A} + \mathrm{COF} \cdot F_n \tag{1}$$

where F_f is the frictional (lateral) force, A is the frictional force at zero-load (which is due to adhesion) and F_n represents the normal force applied. As an example, in Fig. 3 we

report one curve for each kind of test we performed with the corresponding error bars. As evident from Figs. S8-S11 in the Supporting Information, the data dispersion is very narrow, indicating a high reproducibility of the tests. In the top part of Fig. 3, tests performed in dry and humid nitrogen atmosphere for a MoS_2 coating substrate are reported. The bottom part of the graph shows tests performed in the same humidity conditions for a MoS_2 single crystal sample. Results of the linear regressions are also shown within the graphs. The slope and the intercept with the y-axis represent the COF and the contribution due to adhesion of the system.

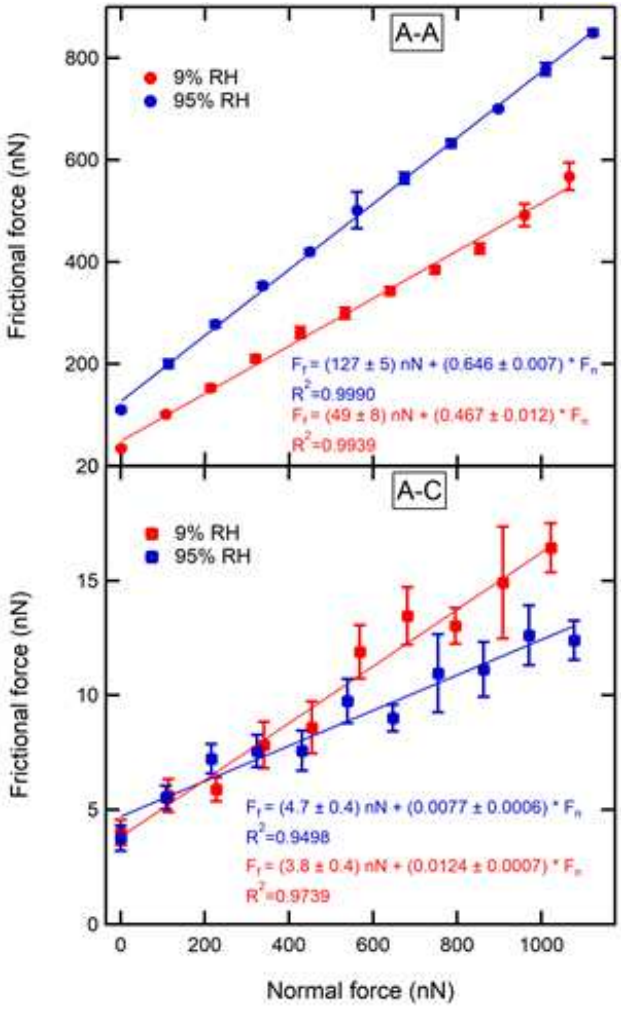

Figure 3: Examples of friction curves obtained for different tests in dry (red curve, RH = 9 %) and humid (blue curve, RH = 95 %) nitrogen atmosphere for a MoS_2 coating (top) and a single crystal (bottom).

This set of parameters was averaged over the four curves reported in Fig. S8 in the Supporting Information for all the different tests performed. The uncertainty was taken as the semidispersion of the data. The average COF for a polycrystalline coating probed in nitrogen atmosphere is 0.41 ± 0.05. The same analysis was performed on the data presented in Fig. S9 of the Supporting Information for measurements obtained on the

same sputter-deposited coating in high humidity atmosphere (RH = 95 %). It resulted in the following parameters, COF = 0.58 ± 0.06. The value of adhesion obtained with this method is characterized by a large uncertainty and, consequently, it does not allow reliable considerations.

The COF measured in dry nitrogen appears to be 50 % lower than in humid air, mimicking what already reported at the macroscale in vacuum and air[54], even if less pronounced.

In the single crystal case the very low value of the lateral force leads to a large associated uncertainty, being close to the detection limit of the system. This peculiarity is partially ascribable to the morphological and mechanical characteristics of MoS_2 single crystal surface, which generates instability in the AFM measurements. In fact, contrary to the case of the very flat and stable surface of sputter-deposited samples, in the case of molybdenite the sample is less rigid and easy-to-exfoliate, generating tilted broken and semi-detached flakes. In order to minimize these phenomena, before each test the MoS_2 single crystal was exfoliated by scotch-tape to have large freshly cleaved regions. We report in Figs. S10 and S11 in the Supporting Information the friction curves obtained respectively in nitrogen and high humidity atmosphere.

The average COF value in nitrogen (COF = 0.0121 ± 0.0017) is very similar to the value obtained in high humidity atmosphere (COF = 0.013 ± 0.005). Our results suggest that the effect of humidity (at least in our range of humidity levels) on friction response of a single crystal MoS_2 is very limited.

Wear of the tip was always monitored via SEM-FEG imaging after tribological tests. Fig. 2b, Figs. S4 and S6 in the Supporting Information suggest that the film did not wear through and that the Si was not exposed: the MoS_2 vs MoS_2 contact were preserved during all the tests performed. The measurement was repeated with different tips coated with 100 nm MoS_2 film, leading to similar results.

4.3. Simulation results

Here we present the results obtained from MD simulations. The A-A and A-C cases show substantial differences in the sliding dynamics. In Fig. 4, snapshots taken along the sliding MD trajectories obtained at an intermediate load are reported (videos reporting the whole MD trajectories are available in the Supporting Information).

For the A-A case a continuous deformation induced by shear (*i.e.*, smooth sliding dynamics) is observed, whilst for the A-C a "stick-slip" mechanism of sliding is instead revealed[55]. A clear slipping interface can be identified for all sliding events (for the trajectory reported in Fig. 4, it comprises the region between the first, second and third crystalline layers starting from the top) and the sliding dynamics consists of jumps between stable states along the sliding coordinate[56]. This behavior can also be highlighted by looking at the motion of the center of mass of the atoms belonging to the top rigid group, as reported in Fig. 5, where discrete slipping events can be easily identified.

Total forces acting on the atoms belonging to the rigid top group along the sliding direction are calculated for all simulated systems. Due to the different features emerging from the A-A and A-C cases, the batch average of the force taken with a window of 50 ps and the total average were used as final values of the frictional force for the former and the latter

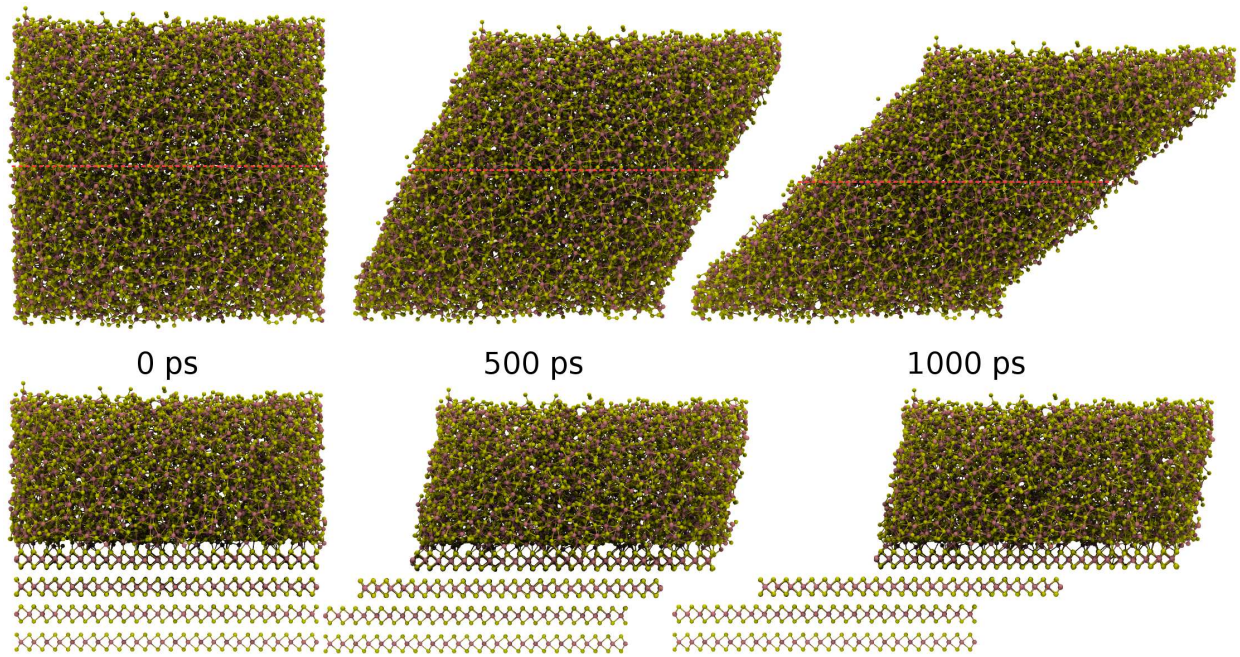

Figure 4: Side view of snapshots taken at the beginning (left), at the midpoint (center) and at the end (right) of example MD trajectories for the A-A (top) and the A-C (bottom) case. Applied normal load is 5 GPa. For the A-A case, the position of the interface is reported with a red dashed line.

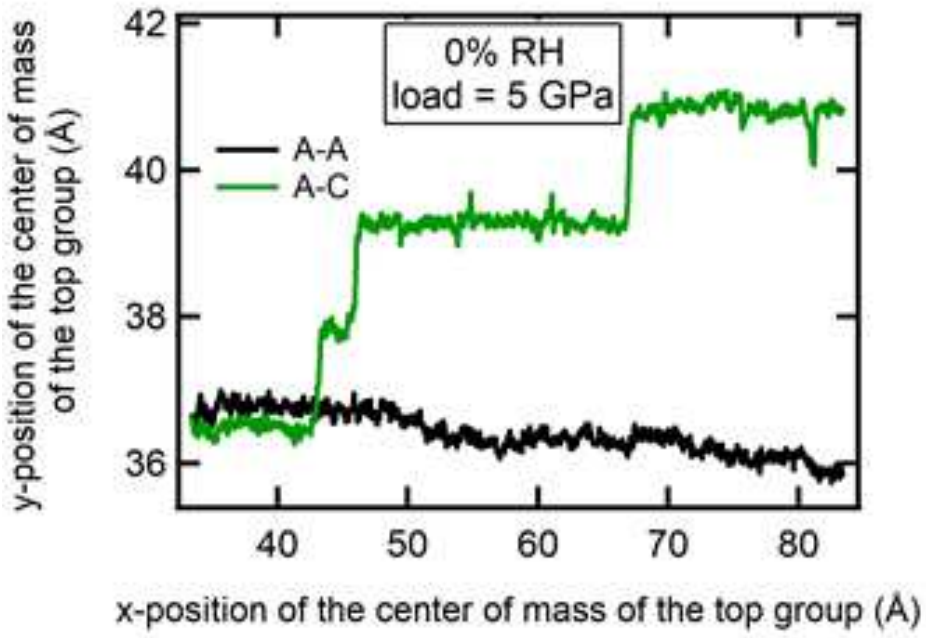

Figure 5: Position of the center of mass of the top rigid layer for an A-A and a A-C trajectory with an imposed load of 5 GPa. For the A-C case, sudden jumps corresponding roughly to one half of the in-plane lattice constant along the y-direction are clearly visible.

case respectively. Finally, for any value of the normal load, we took the average among the five independent trajectories, also calculating the standard deviation of the sample. The results are reported in Fig. 6. Roughly speaking, the trends are linear in both cases (*i.e.*, the systems obey Amontons' law), as already evidenced experimentally, and the A-C setup presents both a lower friction coefficient and a smaller value of the frictional force at zero load. Further comments on the comparison between experimental and computational outcomes are given in the next section.

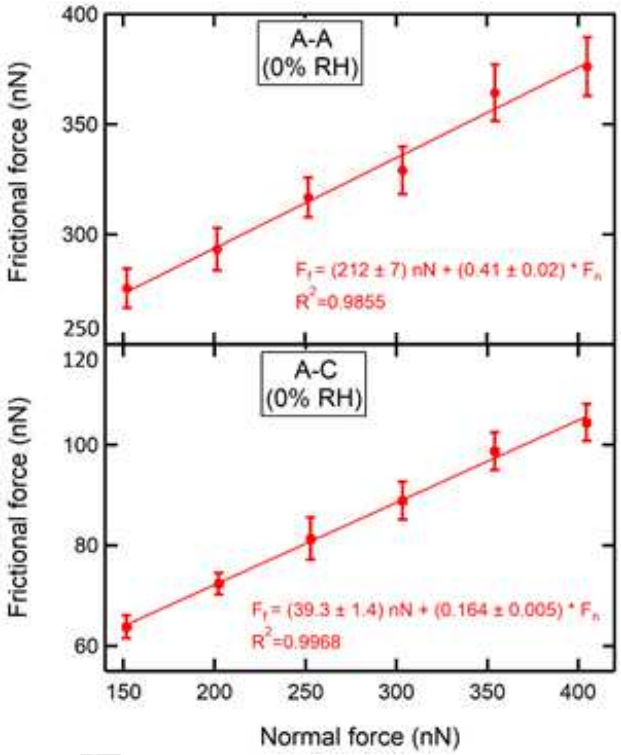

Figure 6: Values of the frictional forces obtained through MD simulations versus the applied normal load for the A-A (top) and A-C (bottom) cases. Standard deviation of the sample made on five independent trajectories are reported as error bars. Results of the linear regressions are also shown within the graphs.

5. Discussion

The friction curves for MoS_2 single crystal corresponding to test in humid ambient and dry nitrogen overlap almost perfectly (see Fig. 3, lower panel). This evidence indicates that the presence of humidity does not influence the tribological behaviour of high-ordered MoS_2, probably related to the fact that in the case of an almost perfectly structure, only very few edges are exposed to water molecules.

Conversely, the slopes of the analogous friction curves for sputter-deposited film are slightly different (see Fig. 3, upper panel). In the case of humid environment, the COF is higher with respect to dry nitrogen case. This can be explained considering that, in the

case of a polycrystalline structure such as the sputter-deposited film, the number of edges is extremely larger with respect to the single crystal case. Consequently, taking into account the larger reactivity of edges with respect to basal planes, water molecules physisorption is much more efficient in the case of the deposited film. This result can be compared with the macroscale. Indeed, it is well known at the macroscopic scale that humidity dramatically influences MoS_2 behavior[1, 9, 11, 23, 28]. However, at the macroscale the reduction of COF in dry and inert environments with respect to humid ones is usually of orders of magnitude. This effect seems to be limited at the nanoscale. It should be mentioned, however, that there is a number of differences between experiments performed at the two scales. For example, in all the studies performed at the macroscale, the counterpart is not previously coated with MoS_2, but gets successively covered by MoS_2 debris or a more adherent tribofilm. Of course, differences in sliding distances, applied loads and pressures, timescales, contact area and even typology of sliding experiment (ball-on-disc, pin-on-disc, reciprocating, etc.) are present as well. We speculate that the differences in contact area and chemistry of the counterpart especially influence the results obtainable at the two scales.

However, the most striking results is represented by the huge difference in the COF measured in dry nitrogen for single crystal and sputter-deposited film, being the former almost 40 times lower than the latter. This means that, at least in dry atmosphere, the role played by the crystallinity of the material is crucial. In order to explain this aspect, the energetics of sliding of amorphous and ordered MoS_2 surfaces needs to be taken into account. In the case of ordered vs ordered layers, the sliding process can be seen as the continuous overcoming of weak van der Waals forces between MoS_2 layers. This simplified scenario is reasonable at the nanoscale, while at the micro/macro-scale other purely dissipative phenomena should be taken into account. In the case of amorphous vs amorphous layers the sliding consists not only in the overcoming of van der Waals forces, but also in the breaking of covalent bonds that continuously form between the two surfaces, due to unsaturated bonds. The energy barriers which correspond to these two scenarios differ two order of magnitude, thus justifying the very different COFs.

The comparison between experimental and MD results can be performed only in inert atmosphere. The agreement is especially good for the COF in the A-A case (see Tab. 1). Although there is perfect agreement on experimental and simulated COF values in

	COF	
System	Experiments	Simulations
A-A	0.41 ± 0.05	0.41 ± 0.02
A-C	0.012 ± 0.002	0.164 ± 0.005

Table 1: Values of friction coefficients for all cases here presented.

the A-A case, in the A-C one the experimental COF is one order of magnitude lower with respect to the one obtained from simulations. It is important to stress that the crystalline material was modeled for the sake of simplicity by assuming ideal commensuration between layers. This means that, during the sliding dynamics, all crystal units need to overcome the energetic barriers simultaneously. This is obviously the most dissipative scenario, and

therefore both the values of the friction coefficient and the contribution of adhesion to friction obtained from MD simulations must be taken as upper limits. This effect is well known in literature[37]. In fact, transmission electron microscopy images obtained from crystalline samples after sliding[19] revealed that a non-zero misfit angle between layer orientation is indeed observed and it leads to the emergence of the superlubric behavior (due to the cancellation of sliding barriers among different regions of the sample[57]). To highlight this effect (*i.e.*, the friction reduction obtainable through lattice incommensuration), sliding MD simulations on accidentally commensurate MoS_2 bilayers were carried on and the results are presented in Section S5 of the Supporting Information, further confirming that rotationally distorted structures show smaller frictional forces than in the commensurate case.

Finally, we will briefly comment here on the validity of Amontons' law. Molybdenum disulfide coatings (prepared by sputtering) can exhibit, under specific conditions, significant deviation from traditional Amontons' law – their friction coefficient decreases with applied load. Singer *et al.*[58] and Grosseau-Poussard *et al.*[59] showed that the friction coefficient decreases with load following COF $\sim F_n^{-1/3}$. The friction change with load is fully reversible, *i.e.* friction increases during unloading. Some experimental studies related this behavior to the decrease of shear strength of MoS_2 under higher pressure[60], but recently published simulations do not support this claim[35]. Higher pressure increases frictional heating in the contact and that may affect interaction with water molecules; however, the decrease of friction with applied load was observed both in humid air and argon[59]. Therefore, the interaction of water molecules with MoS_2 can contribute to the deviation from Amontons' law, but it cannot fully explain such behavior. Our experiments and simulations show that the friction force of both amorphous (A-A) and single crystal (A-C) sliding system is linearly dependent on the load. Therefore, we can suggest here that frictional anomaly observed in macroscopic sliding is likely to be related to re-ordering of MoS_2 basal planes at high contact pressures.

6. Conclusions

Lateral force microscopy and non-equilibrium molecular dynamics simulations revealed details on the frictional behavior of single crystal (ordered) and sputter-coated (disordered) MoS_2 materials. The use of MoS_2-coated atomic force microscopy tips allowed us to study the frictional properties of molybdenum disulfide versus itself, thereby characterizing sliding dynamics taking place within the 2D material itself. Friction experiments at nanoscale revealed that not only the crystalline material exhibits lower values of the friction coefficient than in the disordered case, but also that the crystalline material is less sensitive to humidity and to atmospheric conditions in general. Even though the sliding conditions studied in this paper are far from those in macroscale frictional experiments, our findings can pave the way to the application of MoS_2 coatings with high crystallinity under working conditions different from vacuum. Molecular dynamics simulations corroborated understanding of the phenomena taking place at the nanoscale during the sliding dynamics. The good match between experimental measurements and simulation results obtained for the disordered case allowed us to speculate that, in the ordered case, partial layer incommensuration plays a role

in the friction reduction process. Moreover, this study also evidenced the capability of these molecular dynamics simulations to be a predictive tool allowing assessment of the frictional properties of MoS_2-based materials *in silico* under different tribological conditions.

7. Acknowledgments

This work was supported by the Center of Advanced Applied Sciences CZ.02.1.01/0.0/0.0/16_019/0000778 funded by the European Regional Development Fund (ERDF) and Ministry of Education, Youth and Sports of the Czech Republic. The work was also supported by Large Research Infrastructures: IT4Innovations National Supercomputing Center (LM2015070) and LNSM (LM2011026). We acknowledge PRACE for granting us access to the DECI resource Eagle based in Poland at PSNC with support from the PRACE aisbl. International collaboration on this work was also partly supported by the COST Action MP1303 "Understanding and Controlling Nano and Mesoscale Friction". P.N. acknowledges support from the Czech Science Foundation, project 16-11516Y.

[1] R. Fusaro, Lubrication and Failure Mechanisms of Molybdenum Disulfide Films I – Effect of Atmosphere, Technical Paper 1343, NASA (1978).
[2] R. Fusaro, Lubrication and Failure Mechanisms of Molybdenum Disulfide Films II – Effect of Substrate Roughness, Technical Paper 1379, NASA (1978).
[3] T. Splavins, Lubrication with Sputtered MoS_2 Films: Principles, Operation, Limitations, Technical Memorandum 105292, NASA (1991).
[4] T. Spalvins, A review of recent advances in solid film lubrication, Journal of Vacuum Science & Technology A 5 (2) (1987) 212–219.
[5] M. Hilton, P. Fleischauer, Applications of Solid Lubricant Films in Spacecraft, Surface & Coatings Technology 54-55 (2) (1992) 435–441.
[6] M. Hilton, R. Bauer, P. Fleischauer, Tribological Performance and Deformation of Sputter-Deposited MoS_2 Solid Lubricant Films During Sliding Wear and Indentation Contact, Thin Solid Films 188 (2) (1990) 219–236.
[7] C. Donnet, J. Martin, T. L. Mogne, M. Belin, Super-low Friction of MoS_2 Coatings in Various Environments, Tribology International 29 (2) (1996) 123–128.
[8] V. Fox, J. Hampshire, D. Teer, MoS_2/metal Composite Coatings Deposited by Close-field Unbalanced Magnetron Sputtering: Tribological Properties and Industrial Uses, Surface & Coatings Technology 112 (1-3) (1999) 118–122.
[9] V. Buck, Morphological Properties of Sputtered MoS_2 Films, Wear 91 (3) (1983) 281–288.
[10] T. Jervis, M. Nastasi, R. Bauer, P. Fleischauer, Laser Surface Processing of Molybdenum Disulfide Thin Films, Thin Solid Films 181 (1-2) (1989) 475–483.
[11] J. Lince, M. Hilton, A. Bommannavar, EXAFS of Sputter-deposited MoS_2 Films, Thin Solid Films 264 (1) (1995) 120–134.
[12] T. Polcar, A. Cavaleiro, Self-adaptive Low Friction Coatings Based on Transition Metal Dichalcogenides, Thin Solid Films 519 (12) (2011) 4037–4044.
[13] M. Sgroi, M. Asti, F. Gili, F. Deorsola, S. Bensaid, D. Fino, G. Kraft, I. Garcia, F. Dassenoy, Engine Bench and Road Testing of an Engine Oil Containing MoS_2 Particles as Nano-additive for Friction Reduction, Tribology International 105 (2017) 317–325.
[14] T. Scharf, S. Prasad, M. Dugger, P. Kotula, R. Goeke, R. Grubs, Growth, Structure, and Tribological Behavior of Atomic Layer-deposited Tungsten Disulphide Solid Lubricant Coatings with Applications to MEMS, Acta Materialia 54 (18) (2006) 4731–4743.
[15] P. Stoyanov, J. Fishman, J. L. R. Chromik, Micro-Tribological Performance of MoS_2 Lubricants with Varying Au Content, Surface & Coatings Technology 203 (5-7) (2008) 761–765.

[16] A. Castellanos-Gomez, M. Poot, G. Steele, H. van der Zant, N. Agraint, G. Rubio-Bollinger, Elastic Properties of Freely Suspended MoS_2 Nanosheet, Advanced Materials 24 (6) (2012) 772–775.
[17] J. Theerthagiri, R. A. Senthil, B. Senthilkumar, A. R. Polu, J. Madhavan, M. Ashokkumar, Recent advances in MoS_2 nanostructured materials for energy and environmental applications – A review, Journal of Solid State Chemistry 252 (2017) 43–71.
[18] K. P. Furlan, J. D. B. de Mello, A. N. Klein, Self-lubricating composites containing MoS_2 : A review, Tribology International 120 (2018) 280–298.
[19] J. Martin, C. Donnet, T. L. Mogne, T. Epicier, Superlubricity of molybdenum disulfide, Physical Review B 48 (14) (1993) 10583–10586.
[20] A. Lansdown, Molybdenum Disulphide Lubrication, Elsevier, 1999.
[21] N. Renevier, J. Hamphire, V. Fox, J. Witts, T. Allen, D. Teer, Advantages of Using Self-lubricating, Hard, Wear-resistant MoS_2-based Coatings, Surface & Coatings Technology 142-144 (2001) 67–77.
[22] X. Zhang, F. Jia, B. Yang, S. Song, Oxidation of Molybdenum Disulfide Sheet in Water under in Situ Atomic Force Microscopy Observation, Journal of Physical Chemistry C 121 (18) (2017) 9938–9943.
[23] J. Panitz, L. Pope, J. Lyons, D. Staley, The Tribological Properties of MoS_2 Coatings in Vacuum, Low Relative Humidity, and High Relative-humidity Environments, Journal of Vacuum Science & Technology A 6 (3) (1988) 1166–1170.
[24] X. Zhao, G. Zhang, L. Wang, Q. Xue, The Tribological Mechanism of MoS_2 Film under Different Humidity, Tribology Letters 65 (2017) 64.
[25] B. Windom, W. Sawyer, D. Hahn, A Raman Spectroscopic Study of MoS_2 and MoO_3: Applications to Tribological Systems, Tribology Letters 42 (3) (2011) 301–310.
[26] H. Khare, D. Burris, The Effects of Environmental Water and Oxygen on the Temperature-dependent Friction of Sputtered Molybdenum Disulfide, Tribology Letters 52 (3) (2013) 485–493.
[27] H. Khare, D. Burris, Surface and Subsurface Contributions of Oxidation and Moisture to Room Temperature Friction of Molybdenum Disulfide, Tribology Letters 53 (1) (2014) 329–336.
[28] E. Serpini, A. Rota, A. Ballestrazzi, D. Marchetto, E. Gualtieri, S. Valeri, The Role of Humidity and Oxygen on MoS_2 Thin Films Deposited by RF PVD Magnetron Sputtering, Surface & Coatings Technology 319 (2017) 345–352.
[29] X. Zhao, S. Perry, The Role of Water in Modifying Friction within MoS_2 Sliding Interfaces, ACS Applied Materials & Interfaces 2 (5) (2010) 1444–1448.
[30] F. Gustavsson, S. Jacobson, A. Cavaleiro, T. Polcar, Frictional behavior of self-adaptive nanostructural Mo-Se-C coatings in different sliding conditions, Wear 303 (1-2) (2013) 286–296.
[31] H. Li, J. Wang, S. Gao, Q. Chen, L. Peng, K. Liu, X. Wei, Superlubricity Between MoS_2 Monolayers, Advanced Materials 29 (27) (2017) 1701474.
[32] B. Irving, P. Nicolini, T. Polcar, On The Lubricity of Transition Metal Dichalcogenides: an Ab Initio Study, Nanoscale 9 (17) (2017) 5597–5607.
[33] A. Cammarata, T. Polcar, Tailoring Nanoscale Friction in MX_2 Transition Metal Dichalcogenides, Inorganic Chemistry 54 (12) (2015) 5739–5744.
[34] G. Levita, E. Molinari, T. Polcar, M. Righi, First-principles Comparative Study on the Interlayer Adhesion and Shear Strength of Transition-metal Dichalcogenides and Graphene, Physical Review B 92 (8) (2015) 085434.
[35] G. Levita, A. Cavaleiro, E. Molinari, T. Polcar, M. Righi, Sliding Properties of MoS_2 Layers: Load and Interlayer Orientation Effects, Journal of Physical Chemistry C 118 (25) (2014) 13809–13816.
[36] A. Vakis, V. Yastrebov, J. Scheibert, L. Nicola, D. Dini, C. Minfray, A. Almqvist, M. Paggi, S. Lee, G. Limbert, J. Molinari, G. Anciaux, R. Aghababaei, S. E. Restrepo, A. Papangelo, A. Cammarata, P. Nicolini, C. Putignano, G. Carbone, S. Stupkiewicz, J. Lengiewicz, G. Costagliola, F. Bosia, R. Guarino, N. Pugno, M. Müser, M. Ciavarella, Modeling and Simulation in Tribology Across Scales: An Overview, Tribology International 125 (2018) 169–199.
[37] T. Onodera, Y. Morita, R. Nagumo, R. Miura, A. Suzuki, H. Tsuboi, N. Hatakeyama, A. Endou, H. Takaba, F. Dassenoy, C. Minfray, L. Joly-Pottuz, M. Kubo, J.-M. Martin, A. Miyamoto, A Computational Chemistry Study on Friction of h-MoS_2. Part II. Friction Anisotropy, Journal of Physical

Chemistry B 114 (48) (2010) 15832–15838.
[38] M. Dallavalle, N. Sändig, F. Zerbetto, Stability, Dynamics, and Lubrication of MoS_2 Platelets and Nanotubes, Langmuir 28 (19) (2012) 7393–7400.
[39] A. Ostadhossein, A. Rahnamoun, Y. Wang, P. Zhao, S. Zhang, V. Crespi, A. van Duin, ReaxFF Reactive Force-Field Study of Molybdenum Disulfide (MoS_2), Journal of Physical Chemistry Letters 8 (3) (2017) 631–640.
[40] J. Curry, M. Wilson, H. Luftman, N. Strandwitz, N. Argibay, M. Chandross, M. Sidebottom, B. Krick, Impact of Microstructure on MoS_2 Oxidation and Friction, ACS Applied Materials & Interfaces 9 (33) (2017) 28019–28026.
[41] K. Chenoweth, A. van Duin, W. G. III, ReaxFF Reactive Force Field for Molecular Dynamics Simulations of Hydrocarbon Oxidation, Journal of Physical Chemistry A 112 (5) (2008) 1040–1053.
[42] J. Sader, J. Chon, P. Mulvaney, Calibration of Rectangular Atomic Force Microscope Cantilevers, Review of Scientific Instruments 70 (10) (1999) 3967–3969.
[43] C. Green, H. Lioe, J. Cleveland, R. Proksch, P. Mulvaney, J. Sader, Normal and Torsional Spring Constants of Atomic Force Microscope Cantilevers, Review of Scientific Instruments 75 (6) (2004) 1988–1996.
[44] J. Ruan, B. Bushan, Atomic-Scale Friction Measurements Using Friction Force Microscopy: Part I-General Principles and New Measurement Techniques, ASME Journal of Tribology 116 (2) (1994) 378–388.
[45] B. Bhushan (Ed.), Handbook of Micro/Nanotribology, 2nd ed., CRC Press LLC, 1999.
[46] S. Plimpton, Fast Parallel Algorithms for Short-Range Molecular Dynamics, Journal of Computational Physics 117 (1995) 1–19.
[47] B. Schönfeld, J. Huang, S. Moss, Anisotropic Mean-Square Displacements (MSD) in Single Crystals of 2H- and 3R-MoS_2, Acta Crystallographica Section B B39 (4) (1983) 404–407.
[48] V. Varshney, S. Patnaik, C. Muratore, A. Roy, A. Voevodin, B. Farmer, MD simulations of molybdenum disulphide (MoS_2): Force-field parameterization and thermal transport behavior, Computational Materials Science 48 (1) (2010) 101–108.
[49] S. Nosé, A unified formulation of the constant temperature molecular dynamics methods, Journal of Chemical Physics 81 (1) (1984) 511–519.
[50] W. Hoover, Canonical dynamics: Equilibrium phase-space distributions, Physical Review A 31 (3) (1985) 1695–1697.
[51] C. Yoon, J. Megusar, Molecular Dynamic Simulation of Amorphous Carbon and Graphite Interface, Interface Science 3 (1) (1995) 85–100.
[52] H. Hertz, Ueber die Berührung fester elastischer Körper, Journal für die reine und angewandte Mathematik 92 (1882) 156–171.
[53] S. Bertolazzi, J. Brivio, A. Kis, Stretching and Breaking of Ultrathin MoS_2, ACS Nano 5 (12) (2011) 9703–9709.
[54] A. Rota, E. Serpini, G. Gazzadi, S. Valeri, AFM-based Tribological Study of Nanopatterned Surfaces: the Influence of Contact Area Instabilities, Journal of Physics: Condensed Matter 28 (13) (2016) 134008.
[55] P. Nicolini, R. Capozza, P. Restuccia, T. Polcar, Structural Ordering of Molybdenum Disulfide Studied via Reactive Molecular Dynamics Simulations, ACS Applied Materials & Interfaces 10 (10) (2018) 8937–8946.
[56] P. Nicolini, T. Polcar, A comparison of empirical potentials for sliding simulations of MoS_2, Computational Materials Science 115 (2016) 158–169.
[57] M. Hirano, Superlubricity: a state of vanishing friction, Wear 254 (10) (2003) 932–940.
[58] I. Singer, R. Bolster, J. Wegand, S. Fayeulle, B. Stupp, Hertzian Stress Contribution to Low Friction Behavior of Thin MoS_2 Coatings, Applied Physics Letters 57 (10) (1990) 995–997.
[59] J. Grosseau-Poussard, P. Moine, M. Brendle, Shear Strength Measurements of Parallel MoS_x Thin Films, Thin Solid Films 307 (1-2) (1997) 163–168.
[60] J. Jiang, R. D. Arnell, G. Dixit, The Influence of Ball Size on Tribological Behaviour of MoS_2 Coating Tested on a Ball-on-disk Wear Rig, Wear 243 (1-2) (2000) 1–5.

- Friction of ordered/disordered MoS_2 against itself at nanoscale is measured
- Standard AFM tips were successfully covered with a sputter-deposited MoS_2 film
- Experimental findings are interpreted thanks to molecular dynamics simulations
- Detrimental effects of humidity on friction are less pronounced at nanoscale